Real-Time Human Activity Classification Using Gait Cycle Averaging and Biometric Heuristics

1st Grant Ellison
Computer Science
Loyola Marymount University
Los Angeles, US
gelliso1@lion.lmu.edu

2nd Milla Penelope Markovic
Computer Science
Loyola Marymount University
Los Angeles, US
mmarkov1@lion.lmu.edu

3rd Delaram Yazdansepas
Computer Science
Loyola Marymount University
Los Angeles, US
delaram.yazdansepas@lmu.edu

***Abstract*—The classification of human activities in real-time is an essential task of Human Activity Recognition (HAR). For the deployment of HAR systems on devices like smartphones and smartwatches, it is crucial to ensure their efficiency in terms of time and space. Within the realm of human activity classification, a specific focus lies on the categorization of ambulatory activities, including walking, jogging, and ascending and descending stairs. Activity shapelets, which are geometric patterns representing the dominant pattern in ambulation, are extracted and used for accurate and efficient classification of an incoming time series signal from mobile devices. A trade-off must be made between an extensive training period for extracting shapelets tailored to each individual and the deployment of shapelets trained on a broader population at the expense of accuracy. We propose a novel approach for activity shapelet creation using gait cycle averaging, coupled with a method to partition subjects into training clusters based on biometric similarity. A systematic improvement in accuracy is shown when classifying activity data by leveraging biometric partitioning compared to randomly assigned training clusters. Our findings demonstrate that our methods can be used to deploy pre-trained shapelet libraries, eliminating the need for expensive individual training while maintaining high accuracy.**

***Index Terms*—Classification, Time Series, Human Activity Recognition, Activity Shapelets, Machine Learning, Clustering, Biometrics**

I. Introduction

Accurate and resource-efficient classification systems are necessary for the practical and pervasive use of human activity recognition (HAR) by users. Real-time HAR methods often employ wearable sensors to enable unobtrusive analysis and activity recognition in open environments. These sensors facilitate the capture of relevant data for comprehensive and context-aware activity classification. The ubiquity of sensors in devices like smartwatches and smartphones has revolutionized activity recognition by obviating the necessity for users to wear supplementary devices [1]. Triaxial accelerometers, which are pervasive in these devices, present a favorable foundation for real-time classification due to their information-rich nature and ability to generate a time series signal. Leveraging these sensors makes the challenge of real-time human activity classification a variant of the real-time time series classification task.

One common method of real-time time series classification is the use of time series shapelets - concise geometric representations of the common pattern in a time series. Such approaches are popular due to their simplicity and efficiency, as a shapelet library can be deployed, and a matching algorithm can run in real-time. Shapelet-based approaches to classification were first proposed in [2] and have been a topic of immense interest owing to their accuracy and speed. Time series shapelet extraction typically involves two key components: candidate extraction and search. The conventional approach involves windowed candidate extraction, where a fixed window is slid along the time series, and exhaustive pairwise comparisons are performed during search, to identify potential shapelets. Numerous methods have been proposed to accelerate the shapelet extraction and search problem [3], [4], [5]. These approaches are often focused on either extracting fewer candidates or avoiding computation during search.

Human activity is variable and susceptible to various sources of noise. Each individual exhibits distinct patterns while performing activities, introducing interpersonal variability. Additionally, the uncertainty and unpredictability of the surrounding environment contribute to random variations in movement patterns. Training systems on individual subjects can yield high accuracy in activity classification, but this approach typically incurs a substantial training cost for each individual. An alternative approach involves training systems on a population of subjects, which offers advantages in terms of cost and scalability. However, this approach involves a trade-off, resulting in reduced accuracy and precision compared to individual-specific models. For instance, [6] presents a system able to achieve 94% accuracy when trained on individuals, but only 56% accuracy when trained on a population. This tradeoff is particularly salient for exhaustive shapelet approaches to HAR classification, as a shapelet candidate that is selected as the most representative, on average, of a population, may not be generalizable to subjects whose activity data the shapelet did not come from.

Hierarchical classification systems, as proposed in [7] offer resource-efficient approaches to online classification, avoiding expensive classification tasks when unnecessary. Our work focuses on the classification of ambulatory activities. Ambulatory activities are cyclical, offering natural segmentations based on the gait phase cycle. We envision our system being used within a hierarchical classification system, first identifying that ambulation is occurring, and using our methods to sub-classify which ambulatory activity. To the best of our knowledge, [8] is the only other study that has employed a similar time series shapelet approach for real-time classification of human activity. The focus of their work is on the classification and analysis of individual subjects, utilizing stepped candidate extraction and exhaustive pairwise comparison of shapelet candidates. The use of an exhaustive shapelet search makes this work subject to the aforementioned dilemma between generalizability and accuracy. Consequently, there is no direct comparison between our methods and others in this context.

The major contributions of our paper include an extension of the work presented in [8] by proposing an alternative method for activity shapelet extraction using gait cycle averaging. This novel approach addresses a key challenge encountered by other shapelet-based methods when dealing with training data from multiple subjects. Second, to avoid the training time for each individual, a biometric heuristic is used for partitioning training data before shapelet extraction. This allows common activity shapelets to be used between people with similar biometric profiles, following the basic intuition that a person's gait pattern is influenced by their physical characteristics. Compared to similar approaches that train on individuals, our method, trained on a population, approaches comparable accuracy for real-time activity classification.

The organization of the rest of the paper is as follows: we first give an overview of the data collection protocols and population sample (Section 2). We will then present the biometric partitioning process for delineating subjects into training clusters (Section 3), followed by a detailed explanation of the shapelet extraction and training method (Sections 4 & 5). Section 6 will describe our experiment to show an empirical account of the accuracy of our system. Finally, we will conclude with a summary of our contributions, limitations, and directions for future work.

II. Overview

To improve upon the classification pipeline, a process for partitioning data based on biometrics is presented. Our partitioning system consists of a two-step process. First, a set of biometric data is clustered for each subject, to partition subjects into training clusters. Second, for each partition, times-series activity shapelets are extracted from each activity. The output of the process is a shapelet library for each training cluster, relating to the biometric characteristics of a subject. A shapelet library can be deployed in an online system to classify in real-time, as they are very space efficient. Each shapelet in the library is scored against an incoming signal, and the results are passed through a multi-layer perceptron to provide a final multiclass activity label output.

A. Data Collection

Many HAR datasets contain extensive activity data, or separately, extensive biometrics data. To address the question of the impact the biometrics have on ambulatory activities, and subsequently online classification, it was imperative for us to gather comprehensive activity data, complemented by subject-level biometrics information.

In our study, 35 subjects (20 female, 15 male) had biometrics samples taken. A total of 15 numerical biometrics and an additional 10 qualitative metrics were assessed. Table I shows brief sample statistics from our data collection of the biometrics in the analysis (excluding sex).

TABLE I
SAMPLE STATISTICS

Features	Avg.	Std. Dev.
Age	28	12.0
Height (cm)	171	10.5
Weight (kg)	66	13.5
Dominant Leg Length (cm)	98	7.7
Shoe Size (US)	9	1.8

Subjects wore three wearable sensors (ActiGraph GT9X Link[1]) to collect triaxial accelerometer data (100 Hz, ± 16 g) for a series of 5 activities, on the non-dominant hip, the non-dominant lower shank, and on the non-dominant wrist. Each subject walked on the sidewalk for a set distance, walked up and down a set of stairs, walked on the treadmill at 2.5 mph for 2 minutes, and jogged on the treadmill at 5.5 mph for 1 minute. The analysis is focused on the hip-worn accelerometer. The source code and our full dataset are available [9], [10]

B. Activity Data

From the trivariate time series signal created by the accelerometer, the vector magnitude of the acceleration is created.

$$v_t = \sqrt{x_t^2 + y_t^2 + z_t^2} \tag{1}$$

This improves the robustness of our data against the orientation of the sensor and allows us to easily incorporate information from all three axes while keeping our data as a simple univariate time series.

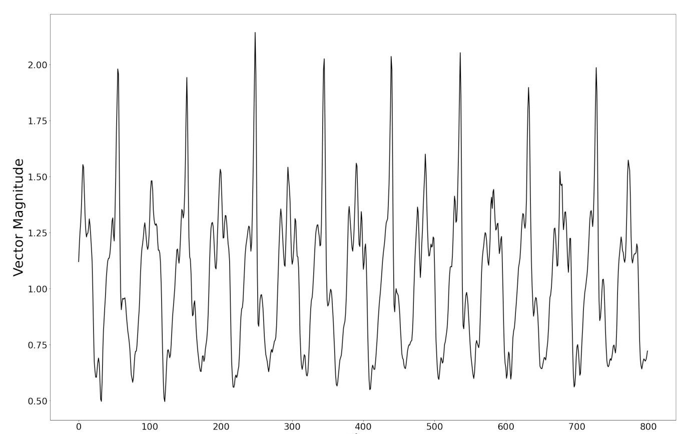

Fig. 1. Eight seconds of sidewalk walking from waist sensor of participant 001.

[1]ActiGraph, LLC, Pensacola, FL, https://theactigraph.com/

Activity data, $a = (v_1, v_2, ..., v_T)$, as shown in Figure 1, is a time series representation of the vector magnitude of acceleration, where T is the number of discrete samples, sampled at 100hz.

III. Biometric Partitioning into Training Clusters

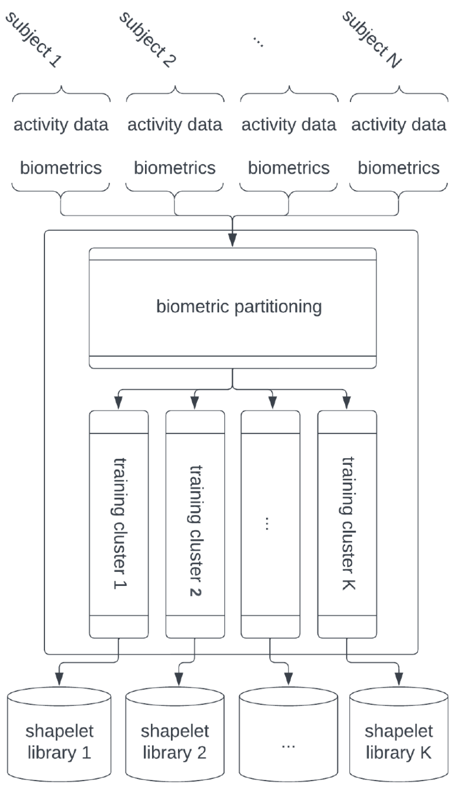

Fig. 2. Overview of the Biometric Partitioning Process

Partitioning our dataset allows us to create more specific shapelet libraries, while still avoiding the individual training period. Subjects are partitioned into training clusters according to biometric similarity.

Clustering is used to identify the similarities present in our subjects' biometrics. Set $B = \{\vec{b_1}, \vec{b_2}, ..., \vec{b_N}\}$ is created where each $\vec{b_n}$ is a vector containing a set of biometrics pertaining to $subject_n$. Centroids $M = \{\vec{m_1}, \vec{m_2}, ..., \vec{m_K}\}$, are initialized by randomly sampling the set B, K times. B is clustered with inertia defined as the sum of the squared distances between each $\vec{b_n}$ and the centroid $\vec{m_k}$ of its assigned cluster C_k. The goal of the clustering algorithm is to minimize the cluster inertia - the distance between each instance s_n and the centroid m_k of its assigned cluster C_k.

$$inertia = \sum_{n=1}^{N} \sum_{k=1}^{K} I(\vec{b_n} \in C_k) |\vec{b_n} - \vec{m_k}|^2 \tag{2}$$

Where N is the number of subjects, K is the number of clusters, and I takes on the value of 1 if $\vec{b_n}$ is a member of cluster C_k, and a value of 0 otherwise. *KMeans* is used to update centroids and assign membership of each $\vec{b_n}$ to a cluster C_k according to Lloyd's algorithm [11]. The initial centroids are resampled 5 times and return the cluster assignment and centroid set that results in the minimum inertia.

The cluster assignment that results from the clustering process is used to partition the data into K training clusters. Figure 2 provides a visual overview of the biometric partitioning process.

IV. Activity Shapelet Extraction

For each $subject_n$ in training cluster k, and for each activity a, a stepped window of a set length is iterated over the activity data. Resampling is done by randomly initializing the starting point until an adequate and fixed number of subsequences are obtained from each person and activity. The final training dataset, for shapelet extraction of training cluster k, consists of a 1-dimensional concatenation of our bootstrapped sampling.

Minimal preprocessing is applied to retain the scale of the extracted shapelets, ensuring their inherent characteristics remain intact. By minimizing preprocessing steps during the training phase, we aim to reduce the computational burden imposed on the real-time classifier during online classification. First, the training activity data $a = (v_1, v_2, ..., v_T)$ is smoothed using a moving average

$$v_t = \frac{1}{p} \sum_{i=t}^{t+p} v_i \tag{3}$$

Where p is the smoothing period maintained as a hyperparameter.

Second, each activity data sequence is centered on the median, which brings the gravitational constant to zero.

$$a = a - \begin{cases} \gamma[\frac{T+1}{2}] & \text{if T is odd} \\ \frac{\gamma[\frac{T}{2}] + \gamma[\frac{T}{2}+1]}{2} & \text{if T is even} \end{cases} \tag{4}$$

Where γ is our activity data, a, reindexed in monotone increasing order, and T is the number of samples.

A. Gait Cycle Extraction

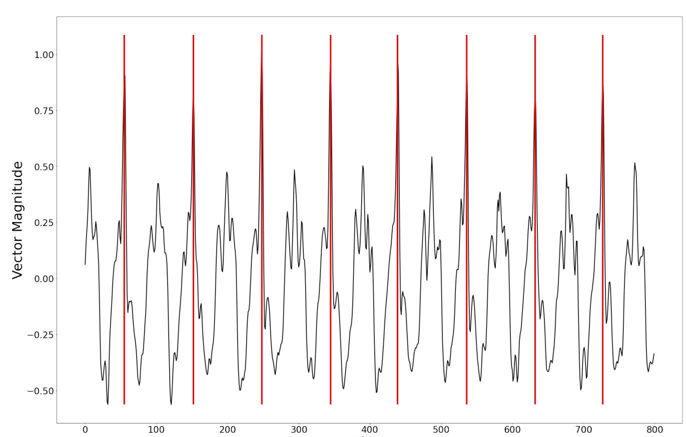

Fig. 3. Peak-finding for gait event detection captures the whole gait cycle from heel-strike to toe-off of the dominant leg.

A gait comprises sequential cycles separated by gait events, most notably the heel-strike, and toe-off [12]. The data was collected in a controlled environment, and labeled by our researchers, therefore a simple, rule-based algorithm is used to extract gait cycles. A peak-finding algorithm, PeakUtils, is used to detect gait events. Figure 3 illustrates the peaks identified by PeakUtils on activity data highlighted in red.

A library of candidate subsequences is created, $C_a = \{c_1, c_2, ..., c_L\}$ where c_l is a gait cycle extracted from the peak-indexing algorithm, and a denotes the activity and L is the number of gait cycles.

B. Gait Cycle Averaging

Barycenter averaging is used to find the spatiotemporal sequence that minimizes the distance between a set of time series. Barycenter averaging allows us to incorporate information from each training subject into the final activity shapelet. As opposed to conducting an exhaustive search, which necessarily selects a shapelet from one individual, barycenter averaging can be trained on a population of subjects. This provides advantages in the generalizability of activity shapelets and allows pre-trained shapelets to be deployed on mobile devices.

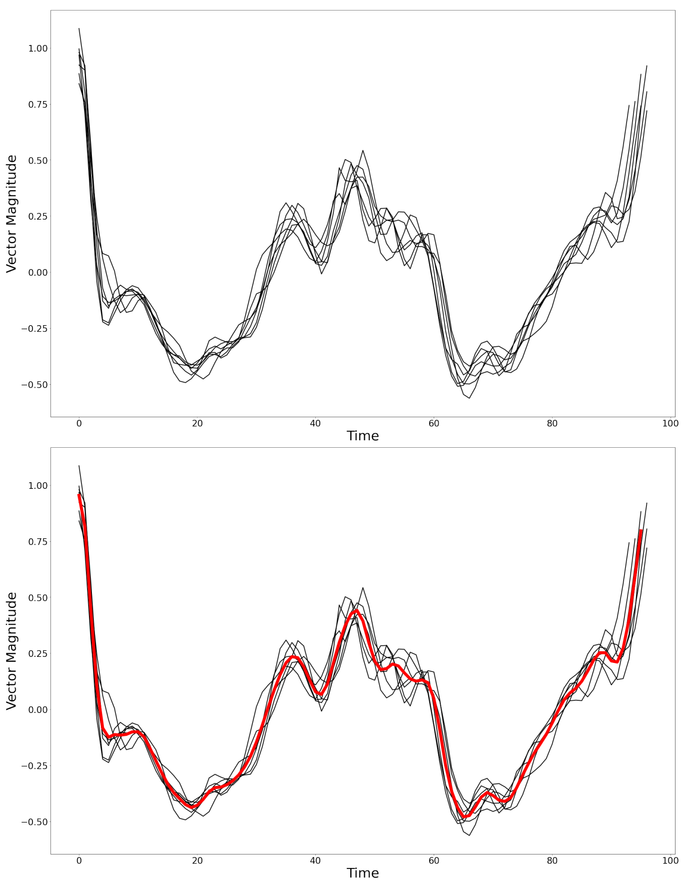

Fig. 4. Above: gait cycle candidate library. Below: an activity shapelet, highlighted in red, created by finding the interpolated average of the candidate library.

DTW Barycenter Averaging (DBA) was proposed in [13], and Soft DTW Barycenter Averaging was proposed in [14]. A simple barycenter averaging technique we call interpolated averaging follows two steps. Given the candidate library $C_a = \{c_1, c_2, ..., c_L\}$, the mean length, μ is found, and each candidate, c_l, is interpolated to a create a vector, $\vec{c_l}$, of length μ. Subsequently, the set of vectors is averaged to obtain a representative value.

$$shapelet_a = \frac{1}{L} \sum_{l=1}^{L} \vec{c_l} \tag{5}$$

where $\vec{c_l} \in \mathbb{R}^{\mu}$. Figure 4 shows an example of interpolated averaging on a gait cycle candidate library. The choice of this method over others is motivated by its notable advantages in terms of simplicity and speed. To enhance the general applicability of DBA, averaging techniques are often employed. Through empirical evaluation of various methods on our dataset, notable enhancements are observed when compared to non-smoothed DBA. Furthermore, our findings demonstrate comparable outcomes between smoothed DBA and interpolated averaging techniques. Figure 4 demonstrates the interpolated averaging technique on our gait cycle candidate library.

Figure 5 shows the final activity shapelets to be deployed for real-time classification. For each shapelet in each $library_k$, the shapelet is repeated so it fits in a window size of four seconds

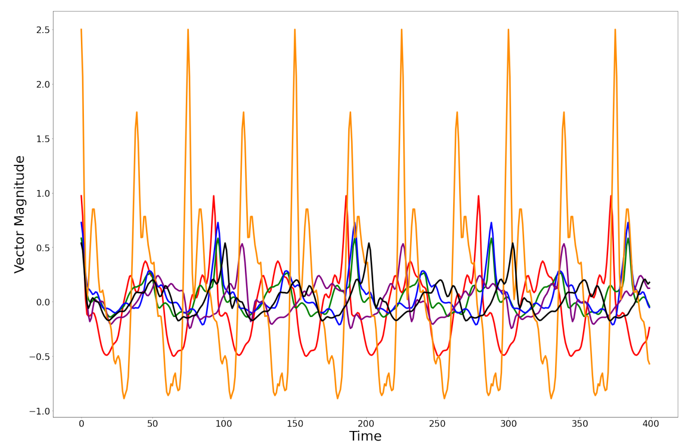

Fig. 5. Library of all activity shapelets for jogging (orange), walking on the treadmill (purple), walking on the sidewalk (red), upstairs (green), downstairs (blue), and mixed-surface walking (black).

Each shapelet library, $library_k = \{s_1, s_2, ..., s_A\}$ consists of an activity shapelet, s_a, for each activity a, where A is the number of activities performed by subjects, and K is the number of training clusters.

V. Classification

Here a real-time multi-class classification system with mutually exclusive categories is presented, that is intended to be used for online HAR systems. A scheme is described for providing a continuous real-time activity classification based on the prior set period of incoming activity data. The system scores each shapelet in the shapelet library against the incoming activity data signal and passes the scores through a multi-layer perceptron for a multi-class output.

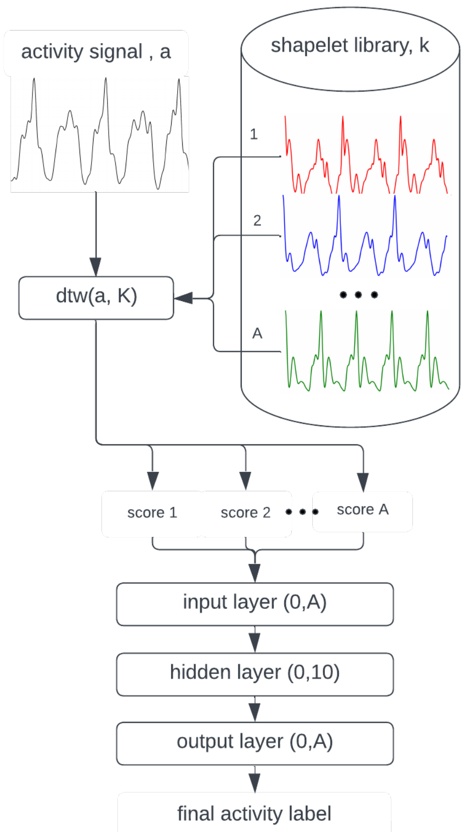

Fig. 6. The classification pipeline scores each activity shapelet against the incoming signal. The vector containing the score of each activity's shapelet is passed as input to a neural network which gives a multiclass output of activity label.

As presented by formulas (3) and (4), incoming data is smoothed using a moving average and center the data on the median. This step holds significant importance for real-time analysis because our system is trained on a group of subjects as a whole, rather than individually.

For comparing two cyclical time series, such as ambulatory activity data, the synchronization of phases in the cycle becomes crucial. The use of certain spatiotemporal distance metrics, such as Dynamic Time Warping, provides some measure of robustness against distortions in time, but another measure is necessary when dealing with incoming signals that may be completely out of phase. The synchronization of our activity shapelets is achieved through our peak finding and gait cycle extraction process. This synchronization ensures that the shapelets are aligned in terms of their phases. To match the incoming signal with the phase of our activity shapelets, again the peak-finding algorithm, PeakUtils is used. The second peak is identified by our algorithm and a subsequencss starting from that point is extracted to the same length as the activity shapelets. This extracted subsequence is then used for scoring purposes.

Dynamic Time Warping (DTW) is a spatiotemporal distance metric used for measuring similarity between time series, especially if the time series is distorted in time [15]. DTW has also been used for gait analysis [12] in other applications. Given an incoming phase-synced activity data signal, $a = \{v_1, v_2, ..., v_T\}$, and our shapelet library $library_k = \{s_1, s_2, ..., s_A\}$, a vector is constructed representing the DTW score of each barycenter in our library compared to the incoming signal.

$$\vec{S} = DTW(a, library_k) \tag{6}$$

$\vec{S}$ is then passed as input into a simple multi-layer perception (MLP), using the Python library, Sci-Kit Learn. The MLP consists of a single, fully-connected hidden layer with 10 neurons. The Rectified Linear Unit (ReLU) activation function is applied within this hidden layer, along with stochastic gradient descent optimization, with a constant learning rate of 0.001. Consequently, this configuration yields our ultimate multiclass output, which consists of the activity labels. It is noteworthy that when implementing the model, the size of the hidden layer should be adjusted according to the number of activities, denoted as A. Figure 6 demonstrates the shapelet scoring and classification process.

VI. Analysis and Results

To evaluate the performance of our classification method, stratified k-fold cross-validation is employed. Three training and testing splits are conducted and the average accuracy from these splits serves as the final performance measure. When assessing the accuracy of the partitioning, we average the results obtained from all the partitions. For calculating the overall accuracy, the accuracy score function provided by Sci-Kit Learn's library is utilized.

A crucial element in the development of a real-time activity classification system is the accurate identification of instances where a subject is engaged in an activity that has not been trained on. To comprehensively evaluate and validate our system, we incorporate a counterfactual scenario. For determining when a subject is performing an activity the system does not recognize, the system is trained on a Gaussian distribution of vector magnitude, with the mean and standard deviation being derived from the training dataset to provide plausible counterfactual activity data. The addition of this random element assesses the system's ability to correctly distinguish trained activities from non-trained activities. It's important to note that the inclusion of this data modestly improves the overall accuracy of our system.

A. Biometric Partitioning

By partitioning our data based on biometrics, training, and validation will occur on a smaller subject population. As a result, a concomitant improvement in performance is expected. To avoid spurious results by assessing the performance of this smaller group, the performance improvement of a dataset trained on partitions made by biometric clustering is compared to a randomly partitioned dataset of similar size.

TABLE II
BIOMETRIC PARTITIONING IMPROVEMENTS OVER RANDOM PARTITIONING

Features	Accuracy	Improvement
Age, Sex	0.85	5.4%
Age, Shoe Size	0.85	5.3%
Sex, Weight	0.84	4.8%
Age	0.84	4.6%
Age, Shoe Size, Height	0.84	4.3%
Age, Sex, Shoe Size	0.84	4.1%
Age, Sex, Shoe Size, Height	0.83	3.7%
Age, Height	0.83	3.7%
Age, Sex, Height	0.83	3.6%

For simplification, $K = 3$ number of training clusters is used, as many biometric subsets tend to create three natural clusters. Partitioning by biometrics creates a 1.3% systematic improvement of accuracy over random partitioning across all biometric sets. It's important to note that this includes sets of biometrics that provide worse than random partitioning results, and there is a heterogeneous effect of biometric partitioning on performance, according to the significance of the biometrics on the gait cycle. An improvement of over 5% is seen among select biometric sets. Table II, shows the performance improvement of the most impactful biometrics.

Upon analyzing Table II;, it becomes evident that age plays a substantial role in the gait pattern. Specifically, when partitioning the data based solely on age, there is a notable improvement of 4.6% compared to random partitioning. This finding suggests age as a significant contributing factor in gait pattern analysis.

B. Efficacy of Different Classification Tasks

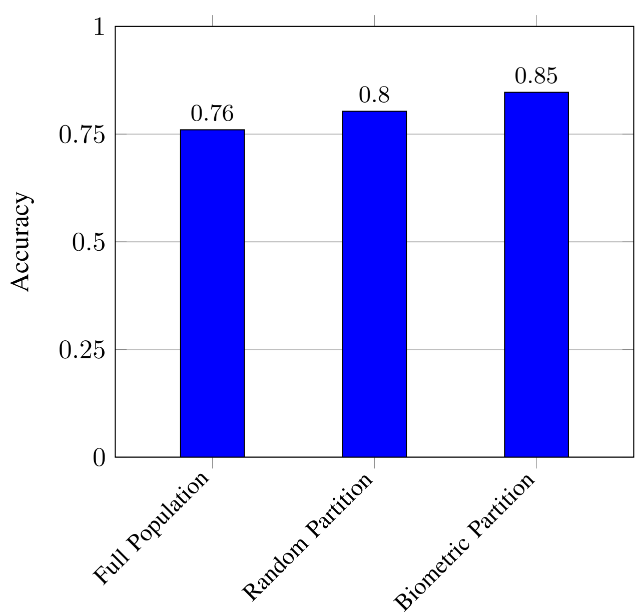

Fig. 7. Accuracy of Multiclass Classification of all Activities - Comparison of Different Training Populations

Here the full account of the accuracy of a system using biometric partitioning is provided. The overall multiclass classification of all activities and some common binary classifications of interest.

Figure 7 demonstrates the difference between training our system on our full sample population of 35 subjects, training on random partitions, and biometric partitions for $K = 3$ training clusters.

As expected, as the size of the training cluster decreases, the accuracy tends to increase. However, by comparing training clusters created by biometric partitioning to those created by random partitioning, biometric partitioning generates superior results.

Figure 8 reports the accuracy of several different classification tasks. As was mentioned earlier, one common approach to online activity classification is hierarchical binary classifications. For this reason, we show the accuracy of our system in classifying whether a subject is walking or jogging, and, if walking, whether they are walking on a treadmill or walking on the sidewalk.

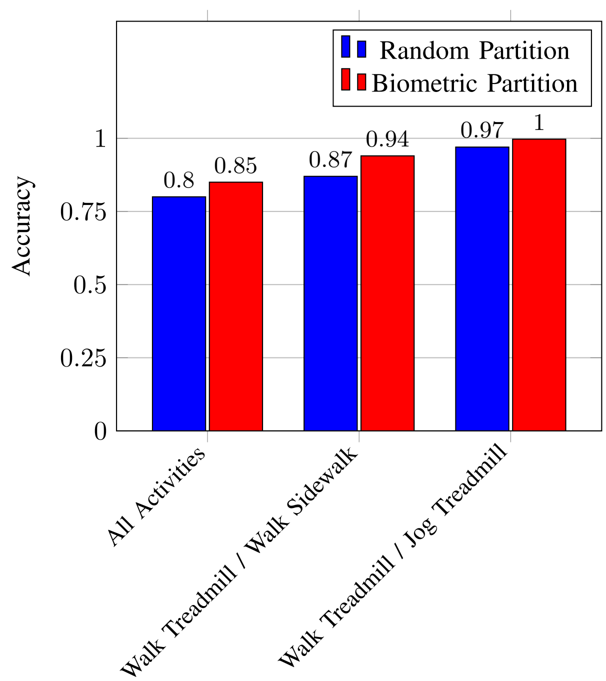

Fig. 8. Accuracy Among Common Classification Tasks - Comparison Between Random Partitioning and Biometrics Partitioning

Once again, biometric partitioning generates a significant improvement over random partitioning. Moreover, taking Table II, Figure 7, and Figure 8 together, this shows that the simplicity of the biometrics that resulted in the most significant improvements demonstrates that systematic improvements can be made with very little input from the user. Age, sex, and shoe size are all characteristics a user knows without the necessity of measurement. Weight and height are additional biometrics that are commonly known.

In their experiments [8] achieved an accuracy level of approximately 86.5% by exclusively training and testing on six individuals. In comparison, our system achieved an 85% accuracy when trained and tested on a population of individuals. This comparison clearly demonstrates the effectiveness of our system in developing pre-trained and generalizable Human Activity Recognition (HAR) systems. Our approach allows us to train a single system on a population, rather than individually for each person, while still achieving comparable accuracy to systems trained on individual subjects.

C. Limitations

Our work primarily focuses on Dynamic Time Warping (DTW) as the sole scoring metric. However, alternative metrics like Euclidean distance, cross-correlation, or approximations of DTW can be employed and examined. Furthermore, the inclusion of additional scoring metrics in our final MLP model could potentially enhance accuracy at the expense of an increase in computational requirements. Further work can be done to validate our methods for sensor independence using smartphones or other types of accelerometers and mobile devices. Our dataset is limited by the need for subject-level biometrics data, but given our findings, other suitable datasets may be used for validation based only on biometrics such as age and sex.

VII. Conclusion

The classification of ambulatory activities is an essential task of human activity recognition. Activity shapelets have been established as a resource-efficient method for real-time classification, but are faced with a tradeoff between the expensive process of training on individuals, or losing accuracy.

To address these issues we offer two solutions. First, we propose gait cycle averaging as an activity shapelet technique, to allow systems to train on a population and deploy shapelet libraries to mobile devices. Second, we show that creating training clusters based on biometric similarity generates systematically better shapelets, in excess of randomly partitioned training clusters. Our results suggest that, with minimal input from users, a system may be trained and deployed for the classification of ambulatory activities in real-time on mobile devices. This opens up possibilities for the pervasive use of HAR systems that are efficient and accurate.

References

[1] O. D. Lara and M. A. Labrador, "A survey on human activity recognition using wearable sensors," vol. 15, pp. 1192–1209. Conference Name: IEEE Communications Surveys & Tutorials.

[2] L. Ye and E. Keogh, "Time series shapelets: a new primitive for data mining," in *Proceedings of the 15th ACM SIGKDD international conference on Knowledge discovery and data mining*, pp. 947–956, ACM.

[3] C. Ji, C. Zhao, S. Liu, C. Yang, L. Pan, L. Wu, and X. Meng, "A fast shapelet selection algorithm for time series classification," vol. 148, pp. 231–240.

[4] X. Renard, M. Rifqi, W. Erray, and M. Detyniecki, "Random-shapelet: An algorithm for fast shapelet discovery," in *2015 IEEE International Conference on Data Science and Advanced Analytics (DSAA)*, pp. 1–10.

[5] A. Mueen, E. Keogh, and N. Young, "Logical-shapelets: an expressive primitive for time series classification," in *Proceedings of the 17th ACM SIGKDD international conference on Knowledge discovery and data mining*, KDD '11, pp. 1154–1162, Association for Computing Machinery.

[6] E. M. Tapia, S. S. Intille, W. Haskell, K. Larson, J. Wright, A. King, and R. Friedman, "Real-time recognition of physical activities and their intensities using wireless accelerometers and a heart rate monitor," in *2007 11th IEEE International Symposium on Wearable Computers*, pp. 37–40. ISSN: 2376-8541.

[7] M. Pedram, S. A. Rokni, M. Nourollahi, H. Homayoun, and H. Ghasemzadeh, "Resource-efficient wearable computing for real-time reconfigurable machine learning: A cascading binary classification," in *2019 IEEE 16th International Conference on Wearable and Implantable Body Sensor Networks (BSN)*, pp. 1–4, IEEE.

[8] D. Yazdansepas, N. Saroha, L. Ramaswamy, and K. Rasheed, "Towards efficient and real-time human activity recognition using wearable sensors: A shapelet-based pattern matching approach," in *13th EAI International Conference on Body Area Networks* (C. Sugimoto, H. Farhadi, and M. Hämäläinen, eds.), pp. 115–130, Springer International Publishing. Series Title: EAI/Springer Innovations in Communication and Computing.

[9] G. Ellison, "https://github.com/gellison321/tsclassification," 2023.

[10] G. Ellison, M. P. Markovic, and D. Yazdansepas, "https://github.com/Har-Lab/HumanActivityData," 2023.

[11] S. Lloyd, "Least squares quantization in PCM," vol. 28, pp. 129–137, IEEE.

[12] S. R. Dandu, M. M. Engelhard, M. D. Goldman, and J. Lach, "Determining physiological significance of inertial gait features in multiple sclerosis," in *2016 IEEE 13th International Conference on Wearable and Implantable Body Sensor Networks (BSN)*, pp. 266–271, IEEE. event-place: San Francisco, CA, USA.

[13] D. Schultz and B. Jain, "Nonsmooth analysis and subgradient methods for averaging in dynamic time warping spaces," vol. 74, pp. 340–358.

[14] M. Cuturi and M. Blondel, "Soft-DTW: a differentiable loss function for time-series," in *Proceedings of the 34th International Conference on Machine Learning*, pp. 894–903, PMLR. ISSN: 2640-3498.

[15] P. Senin, "Dynamic time warping algorithm review," *Information and Computer Science Department University of Hawaii at Manoa Honolulu, USA*, vol. 855, no. 1-23, p. 40, 2008.